Microstructural and Compositional Gradients in the Filament-Matrix Region of Nb-Ti Wire Composites

Kenneth J. Faase and William H. Warnes
Department of Mechanical Engineering, Oregon State University
Corvallis, OR 97333 USA

Peter J. Lee and David C. Larbalestier
Applied Superconductivity Center, University of Wisconsin-Madison
Madison, WI 53706 USA

Abstract—**Transverse cross-sections of Nb-Ti wire composites after final α-Ti precipitation heat treatment (10-480hr/420°C) were examined and analyzed in the filament-matrix region with Scanning Electron Microscope-Backscatter Electron Imaging (SEM-BEI) and Electron Micro Probe Analysis (EMPA). SEM-BEI micrographs were image analyzed to quantify the average effective α-Ti precipitate diameter, d*, and volume fraction of α-Ti as a function of distance into the filament. Cu concentration profiles were found in the same regions by EMPA. The compositional results show trace amounts of Cu (>0.1at%) interdiffused up to 50μm into the Nb-Ti filaments. The interdiffused Cu at the interface increased α-Ti nucleation and thus increased α-Ti volume fractions by 50% relative to the nominally pure Nb-Ti at the center of the filament for short heat treatment times (30 hours of total heat treatment time).**

I. Introduction

In recent years a direct relationship between the critical current density, J_c, and the microstructure of Nb-Ti composites has been developed [1]-[3]. The current density of the Nb-Ti has a strong, linear dependence on the volume percent of α-Ti existing after the final heat treatment. The optimized microstructure of Nb-Ti wires is developed by a series of heat treatments and wire drawing steps. The small α-Ti precipitates (10-250nm), which exist after the final heat treatment, are then drawn into 1-5nm thick ribbons by a final wire drawing strain of 4 to 5. The α-Ti ribbons act as the principal flux pinning sites for the fluxoid lattice.

We recently discovered [4] that the average size of the α-Ti precipitates near the filament perimeter is smaller than the precipitates found at the center of the filament in some Nb-Ti wires at their final heat treatment stage. This variable precipitate size is easily visible with a Scanning Electron Microscope in Backscatter Electron Imaging (SEM-BEI) mode. Due to the simplicity of sample preparation and the ability to choose specific viewing regions anywhere within the filament, the use of the SEM-BEI technique is here further investigated as a useful tool for precipitate quantification.

II. Experimental Procedure

The composites (Table I) in this study were two series of previously studied monofilamentary and multifilamentary Nb46.5wt%Ti wires [4]-[6]. The samples all had excellent J_c values (>2700 A/mm^2 at 5T, 4.2K) and had been well studied microstructurally by transmission electron microscopy (TEM) [7].

Manuscript received October 17, 1994. This work was supported by the U. S. Department of Energy under Grants No. DOE-FG06-93ER40804 and No. DE-AC02-82ER-4007, Teledyne Wah Chang Albany and the Oregon Metals Initiative.

TABLE I
COMPOSITE DETAILS

Composite ID	Description	Heat Treatments	J_c	Plot Symbol [b]
CB2123	Monofilament No Nb wrap	3X10hr/420°C	2764[a]	●
CB2133	Monofilament No Nb wrap	3X40hr/420°C	3231	▲
CB2163	Monofilament No Nb wrap	3X120hr/420°C	3600	■
CB2153	Monofilament No Nb wrap	3X160hr/420°C	3616	◆
5263-3-C	Multifilament Nb wrap	3X80hr/420°C	3196	○
UW6401C	Multifilament Nb wrap	2X80hr/420°C + 1X480hr/420°C	na	❑

[a] J_c measured at 4.2K, 5T.
[b] Plot symbols are used in Fig. 3 and Fig. 4.

Transverse cross sections of the heat treated wires were mounted and polished in conductive bakelite for the electron microscopy. All samples were examined after their final α-Ti precipitation heat treatment. SEM-BEI micrographs of the samples were taken at 10,000 times magnification using a JEOL 35C SEM operating at 20kV and an objective aperture of 240μm. Compositional gradients of the samples were performed on a Cameca SX50 electron microprobe at an accelerating voltage of 15kV and 50nA. The $Cu_{K\alpha 1}$, $Ti_{K\alpha 1}$, and $Nb_{L\beta 1}$ peaks were analyzed for 30, 10 and 10 seconds respectively. One Electron Micro Probe Analysis (EMPA) sample was etched (H_2O:HNO_3, 5:1 by volume) for 60 seconds to check for any residual Cu on the Nb-Ti due to polishing. The etched sample showed no significant change in the EMPA profile relative to its unetched state.

The α-Ti precipitates in the SEM-BEI micrographs were quantitatively analyzed for both volume fraction and average effective precipitate diameter, d*, with image analysis. The micrographs were scanned into a Macintosh IIci with a video digitizer at a resolution of ~16nm/pixel and 256 grey scales. The image analysis was performed on a modified version of NIH Image 1.49 [8].

Due to the large electron beam-specimen interaction volume at 20kV, the α-Ti precipitates in the SEM-BEI micrographs were diffuse in nature. To accommodate the diffuse precipitate boundaries, an image analysis algorithm was developed to locally transform the 256 grey scale map into linear-regression curve fits in order to statistically calculate local precipitate boundaries.

The algorithm scanned the 256 grey scale image for local minimums in image intensity (black: image intensity = 0, white: image intensity = 255) with a user defined kernel size. Each minimum point was marked and accepted or rejected by the user as a valid precipitate signal or as signal noise.

Each of the user accepted local minima then became the

1051-8223/95$04.00

origin for a local polar coordinate system (Fig. 1). The algorithm radially scanned the grey scale intensity, I, as a function of sub-pixel, polar position, (r,θ). The scan went from the local minimum point, in one pixel length increments, to a local maximum on the grey scale surface. The grey scale value of $I(r,\theta)$ was linearly interpolated, at sub-pixel precision, as a function of position and grey scale intensity between (r,θ) and its nearest four neighboring pixels. The distance between the local minimum and maximum was then divided into twenty, equi-distant, sub-pixel precision lengths, r_n. A grey scale intensity array, $I(r_{n=1 \text{ to } 20},\theta)$, was then calculated in the same manner as $I(r,\theta)$.

A fifth order linear regression fit, $I_{fit}(r,\theta)$, was calculated for every intensity array, $I(r_{n=1 \text{ to } 20},\theta)$. The maximum in the gradient of $I_{fit}(r,\theta)$ was then taken as the effective radius, $r^{\dagger}$, of the precipitate at the angle θ. The angle θ was incremented by a user defined $d\theta$, and a sub-area, dA, was calculated as $(1/2)(r^{\dagger})^2 d\theta$. The total area of the precipitate was then found by calculating $r^{\dagger}(\theta)$ and $dA(\theta)$ for all θ from 0 to 2π and summing the sub-areas.

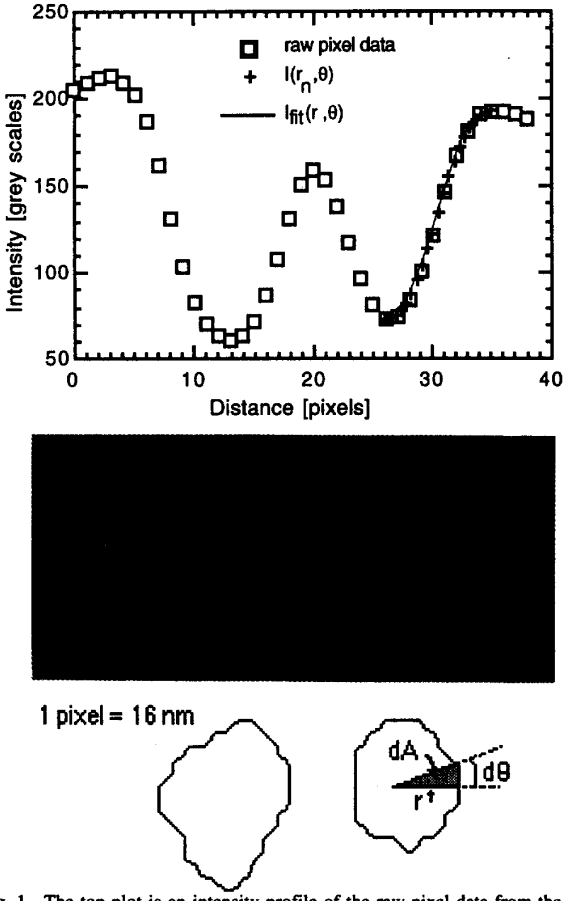

Fig. 1. The top plot is an intensity profile of the raw pixel data from the white line crossing the grey scale image of two precipitates in the middle figure. Also included in the plot is a radial array $I(r_{n=1 \text{ to } 20},\theta)$ and a regression fit $I_{fit}(r,\theta)$ represented by the triple-black/white line on the grey scale image. The bottom figure shows the perimeter of the two precipitates as calculated by the algorithm, as well as a schematic of $r^{\dagger}$, $d\theta$ and dA.

Finally, the algorithm produced a binary image of the calculated perimeters of the precipitates. The binary image was overlaid upon the original 256 grey scale map to check the integrity of the calculation.

From each sample, four 5μm X 5μm areas were image analyzed in the center of the filament. To measure the microstructural gradients, two to four 2.5μm X 2.5μm areas were analyzed in ~2μm spacings from the perimeter towards the center of the filament. EMPA traces were taken in the same regions to complement the microstructural measurements.

III. Results

A comparison of the microstructures at the center and the edge of a filament is shown in Fig. 2. The micrographs confirm the average α-Ti precipitate diameter is smaller at the filament perimeter than at the filament center as suggested in [4]. Although an apparent change in d* exists, no qualitative change in volume fraction of α-Ti is noticeable between the two regions.

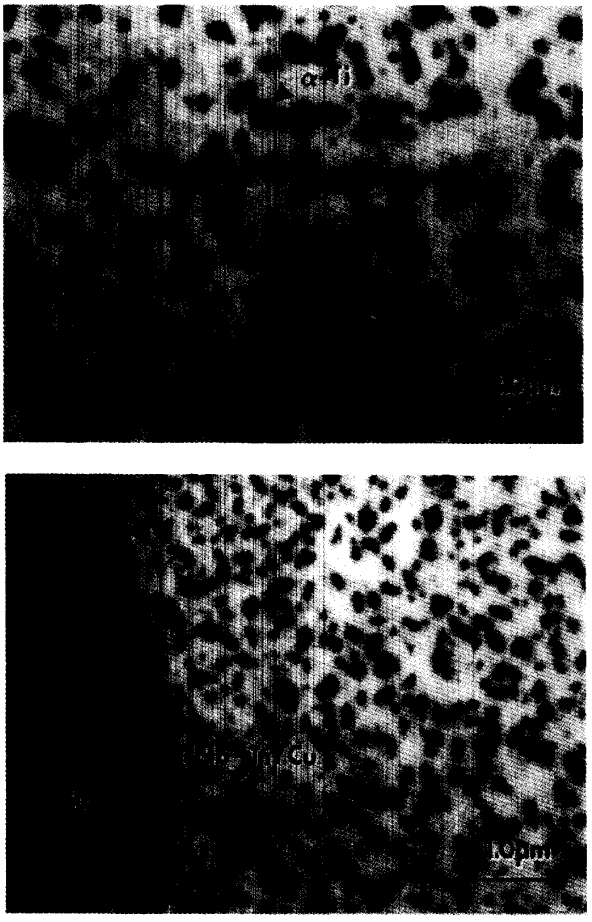

Fig 2. SEM-BEI micrographs of the CB2163 sample after final precipitation heat treatment. The center and perimeter regions of the filament are shown in the top and bottom micrographs respectively. Intermetallic compound can be seen at the filament-matrix perimeter.

Quantitative microstructural profiles of the two regions are shown in Fig. 3. Fig. 3a depicts d* as a function of distance from the filament-matrix interface for the six samples. The d* profiles are a function of total heat treatment time. The UW6401C sample, with a total heat treatment time of 640hr/420°C, has an ~25% reduction in d* from the center of the filament to the filament perimeter. Both the CB2123 and CB2133 samples, with total heat treatment times of 30 and 120 hours at 420°C, respectively, have flat d* profiles.

The volume fraction of α-Ti profiles, Fig. 3b, are also dependent on the total heat treatment time of the sample. In this case, the volume fraction profiles have significant changes, from the filament perimeter to center, only in the samples with low total heat treatment times. CB2123 and CB2133 have α-Ti volume fraction increases of ~50% from the filament perimeter relative to the filament center, while UW6401C has a flat volume fraction profile.

EMPA traces of the filament-matrix regions are shown in Fig. 4. In the samples with no Nb wrap, CB2123 and CB2153, the profiles are again a function of the total heat treatment time of the sample. CB2123, with 30 hours of total heat treatment time, has Cu traces (>0.1at%) up to 20 microns into the Nb-Ti filament, while CB2153, with 480 hours of total heat treatment time, has Cu traces up to 50 microns into the filament. In the two samples with Nb wraps, 5263-3-C and UW6401C, the Cu profiles are similar to each other (as well as similar to the trace for CB2153) yet the total heat treatment times are different by more than a factor of two.

The volume fraction of α-Ti at the center and the perimeter of the filament is plotted against total heat treatment time in Fig. 5. The figure shows that the volume fraction of α-Ti is higher in the perimeter region than in the center region of the Nb-Ti filament for total heat treatment times of less than ~200 hours. After 200 hours of total heat treatment time, both the center and perimeter regions begin to saturate with ~20-25 volume percent of α-Ti precipitate.

The number density of α-Ti precipitates, ρ, of each composite is estimated as

$$\rho = \left[\frac{4 v_{\alpha - Ti}}{\pi d^{*2}} \right] \quad (1)$$

where $v_{\alpha\text{-}Ti}$ is the volume fraction of α-Ti. The estimated number densities are listed in Table II. In all of the samples, except CB2133, the number density of α-Ti precipitate is higher at the filament perimeter than at the center region.

IV. Discussion

The newly developed SEM-BEI microstructural quantification technique has been applied to a simple thermal study. An advantage of this technique relative to TEM examination is the ability to freely choose a region of interest, where the TEM is limited by the available thin area of the sample. This has provided new insights on the microstructural-processing relationship in these composites which has not been possible with the TEM [9].

The presence of Cu in the Nb-Ti, which increases the nucleation rate of the α-Ti precipitates, may offer modest benefits to the performance of the Nb-Ti composites in two possible ways. First, the volume fraction of α-Ti in the

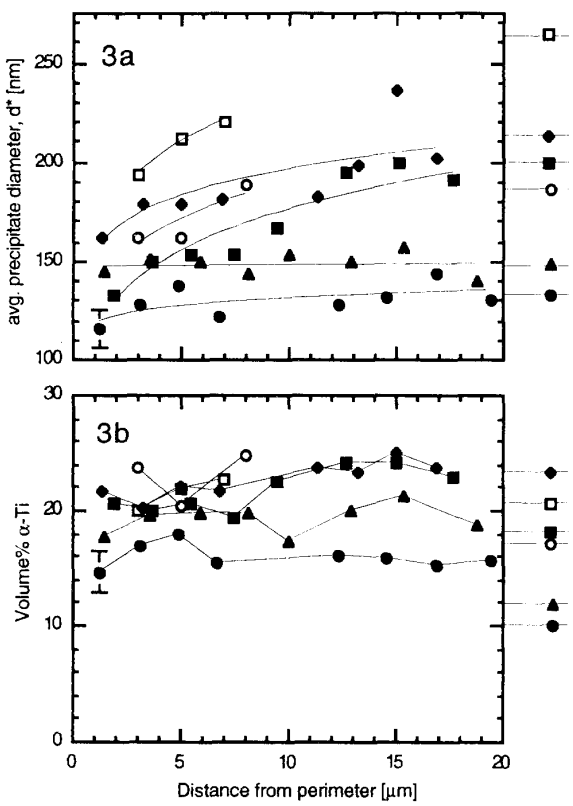

Fig. 3. Microstructural profiles, d* (3a) and volume fraction of α-Ti (3b), of the six samples listed and identified in Table I. The lines and symbols at the right hand side of the graphs represent the measurement of the microstructure at the center of the filament for each sample. Each data point is the average of several measurements, with the error bar in each graph representing a typical standard deviation of the average.

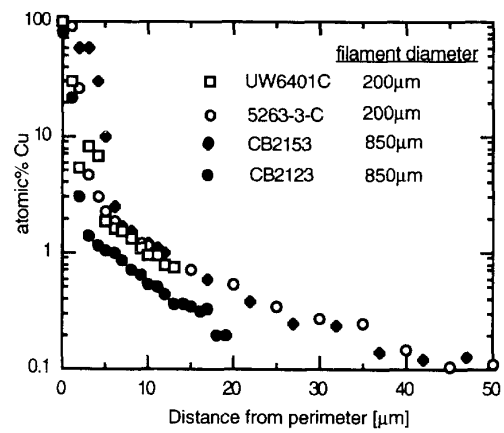

Fig. 4. EMPA Cu profiles. Both UW6401C and CB2153 show intermetallic peaks within 5μm of the filament-matrix interface. The detection limit for Cu is ~0.1at%Cu.

TABLE II
NUMBER DENSITY OF α-Ti PRECIPITATES

Composite ID	Total Heat Treatment Time[hr]	ρ, Filament Perimeter [#/μm^2]	ρ, Filament Center [#/μm^2]	Percent Difference
CB2123	30	15.2±3.6	7.3±2.8	52
CB2133	120	11.3±1.5	6.9±3.8	(ns)
5263-3-C	240	11.5±1.2	7.4±2.6	36
CB2163	360	15.7±4.4	5.6±1.7	64
CB2153	480	12.4±3.1	6.6±1.8	47
UW6401C	640	7.52±2.46	3.68±1.36	51

(ns) This result was statistically non-significant.

regions containing Cu is higher than the regions containing no Cu for total heat treatment times of 200 hours and less. The additional precipitate should provide additional pinning sites for the fluxon lattice, thus increasing J_c. Second, for total heat treatment times of 200 hours of more, the decrease in d*, due to the presence of Cu, should reduce the amount of final strain needed to reach peak J_c.

On the other hand, Cu may be detrimental to the overall superconducting properties of Nb-Ti composites. Reference [10] studied the structure and superconducting properties of prepared Ti60wt%Nb alloys containing trace amounts of Cu. Although they confirm increased nucleation of the α-Ti precipitate with trace amounts of Cu, they also find that the alloys with Cu exhibit reduced T_c. Additionally, reduced superconducting electron energy gaps have been found in Nb-Ti wire composites containing up to 3wt%Cu [11].

Whether beneficial or detrimental, the "Cu-poisoned" zone will play a larger role as the development of conventionally processed wire composites strives for smaller Nb-Ti filament diameters. The 50μm thick layer of Cu contamination (>0.1at%) in the CB2153 and 5263-3-C samples represent ~22% and ~75% of the cross sectional area of the filaments in these conductors, which have final filament diameters of 85 and 20μm, respectively. Wire composites with final filament diameters of ~10μm or less, processed in a similar manner, should have their entire cross sectional area contaminated with 0.1at%Cu or greater.

The extent of the Cu interdiffusion through the Nb wrap was an unexpected result of this study. Qualitatively, 5263-3-C had no signs of the "Cu-poisoned" zone and it was thought to take over 400 hours for the Cu to cross the Nb barrier in the sample [4]. Yet the sample had Cu contamination up to 50μm into the Nb-Ti filament which produced a higher number density of α-Ti precipitates at the perimeter than the center of the filament.

It appears that Cu does not see a substantial barrier to interdiffusion through the Nb wrap until concentrations reach a level high enough to form Cu-Ti intermetallics (>10at%Cu). This would suggest that the Cu is readily diffusing along the grain boundaries of the Nb wrap and Nb-Ti filament, in these heavily deformed composites, until the Cu-Ti intermetallic compound has formed. The intermetallic layer then acts as a sink for additional interdiffused Cu, thus leaving the profile of the trace amounts of Cu in Nb-Ti effectively stationary.

Finally, although the SEM-BEI technique has proven to be quite useful in this study and in quantifying the microstructure in Nb-Ti Artificial Pinning Center (APC) materials [12], it cannot fully replace the TEM

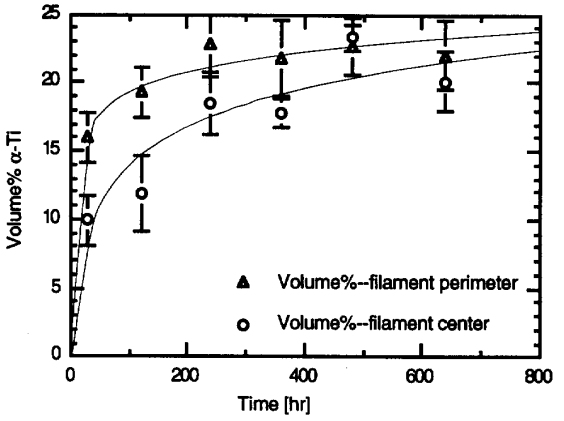

Fig. 5. Volume fraction of α-Ti versus total heat treatment time. Each perimeter point and error bar represents the average and standard deviation of the volume fraction measurements in the first 20μm of the filament-matrix region as shown in Fig. 3. Each center point is simply the average and standard deviation of four measurements made at the center of the filament.

microstructural quantification technique. The SEM-BEI quantification technique is ultimately limited by the electron beam-specimen interaction volume to a resolution of ~10nm. Ideally, this technique should be able to quantify microstructures with an average, gaussian-distributed particle diameter of ~25nm and still have volume (area) fraction measurements accurate within 5% of the TEM. In practice, this average precipitate diameter limit has been found to be more on the order of ~50nm. This excludes the SEM-BEI technique from quantifying the microstructure of these Nb-Ti composites in both their earliest and final microstructural-processing stages, where the α-Ti precipitate is in the form of grain boundary films or ribbons.

ACKNOWLEDGMENT

We would like to thank Rick Noll for his help on the SEM and Roger Nielsen for his assistance on the EMPA.

REFERENCES

[1] P. J. Lee, J. C. McKinnell, and D. C. Larbalestier, *Adv. Cryo. Eng.*, vol. 36, pp. 287-294, 1990.
[2] P. J. Lee, J. C. McKinnell, and D. C. Larbalestier, *Adv. Cryo. Eng.*, vol. 40A, pp. 725-732, 1994.
[3] O.V. Chernyi, et al., *Superconducting Science & Tech.*, vol. 4, pp. 318-323, 1991.
[4] K. J. Faase, P. J. Lee, J. C. McKinnell, and D. C. Larbalestier, *Adv. Cryo. Eng.*, vol. 38, pp. 723-730, 1992.
[5] Li Chegren and D. C. Larbalestier, *Cryogenics*, vol. 27, pp. 171-177, 1987.
[6] Y. E. High, P. J. Lee, J. C. McKinnell, and D. C. Larbalestier, *Adv. Cryo. Eng.*, vol. 38, pp. 647-652, 1992.
[7] P. J. Lee, "Superconducting Materials: Fabrication and Process Variables", SSCL/Industry Technology Transfer, June 1991.
[8] NIH Image is a public domain software package available via the INTERNET @ ftp.soils.umn.edu.
[9] K. J. Faase, M.S. thesis, University of Wisconsin-Madison, 1992, (available from University Microfilms, Ann Arbor, Michigan).
[10] V. A. Vozilkin, T. L. Trenogina, S. B. Volkova and V. P. Korzhov, *Fiz. metal. metalloved.*, vol. 6, pp. 183-187, 1991.
[11] J. Moreland, J. W. Ekin, and L. F. Goodrich, *IEEE Trans. Mag.*, vol. 23, pp. 1101, 1985.
[12] L. D. Cooley, Ph.D. thesis, University of Wisconsin-Madison, 1993, (available from University Microfilms, Ann Arbor, Michigan).